

## Original Article

# Roles of miR-433-5p in gastric carcinoma cell viability, invasion, and apoptosis via targeting CLCN4 genes

Wei Wang<sup>1</sup>, Jing Pan<sup>2</sup>, Hai-Bing Jiang<sup>3</sup>

<sup>1</sup>Oncology Hematology Department, The Second Hospital University of South China, Hengyang, China; <sup>2</sup>Department of Pathogenic Biology and Immunology, Yongzhou Vocational Technical College, Yongzhou, China; <sup>3</sup>Department of Gastroenterology, The Second Hospital University of South China, Hengyang, China

Received March 29, 2019; Accepted June 10, 2019; Epub August 15, 2019; Published August 30, 2019

**Abstract:** Objective: The current study was designed to explore the mechanisms in which miR-433-5p affects viability, invasion, and apoptosis of gastric cancer cells via targeting CLCN4. Methods: Gastric cancer tissues and adjacent tissues were collected. Bioinformatics tools and dual-luciferase reporter assays were utilized to confirm target genes of miR-433-5p. H&E staining was adopted to detect the histopathologic structure. CLCN4 expression was determined by immunohistochemistry. Gastric cancer cell lines with the highest protein expression of CLCN4 were selected for the experiments. Cells were transfected with miR-433-5p mimics, miR-433-5p inhibitors, or CLCN4 shRNAs. A negative Control (NC) group was also set up. Cell viability and invasion abilities were evaluated using CCK-8 and Transwell assays. Q-PCR and Western blotting were used to quantify mRNA and protein expression levels of vimentin and MMP-2. Annexin V-FITC/PI staining was used to detect apoptosis levels of gastric cancer cells. Results: Results obtained from bioinformatics analysis and dual-luciferase reporter assays revealed that CLCN4 was the target gene of miR-433-5p. Immunohistochemical staining results indicated that, compared with para-cancerous tissues, expression of CLCN4 was significantly upregulated in cancer tissues. Cell experiments indicated that, compared with the NC group, cell viability, invasion, and metastasis were downregulated in the miR-433-5p mimics group and CLCN4 shRNA group. MMP-2 and vimentin mRNA and protein expression levels were also decreased, while cell apoptosis was induced in those two groups (all  $P < 0.05$ ). Compared with the NC group, cell viability, invasion, and metastasis levels in the miR-433-5p inhibitor group were significantly upregulated. Moreover, mRNA and protein expression of MMP-2 and vimentin levels were increased. Cell apoptosis was inhibited (all  $P < 0.05$ ). Conclusion: Findings obtained in the current study suggest that miR-433-5p functions as a tumor suppressor through targeting CLCN4 genes, resulting in the inhibition of cell viability, invasion, and metastasis.

**Keywords:** miR-433-5p, CLCN4, gastric cancer, cell viability, invasion and metastasis

## Introduction

Gastric cancer, derived from gastric mucosal epithelium, is one of the most prevalent cancers worldwide [1]. Its characteristic low cure rate has greatly troubled doctors [2]. Despite diagnosis and treatment strategies improving continuously, 5-year survival rates for advanced gastric cancer patients remain very low [3, 4]. Studies concerning the potential molecular mechanisms of this disease are necessary to provide effective therapeutic strategies for gastric cancer patients.

MicroRNAs, as master regulators of several essential cell biological processes, such as cell transcription, apoptosis, cell cycle regulation,

metabolism, and proliferation, have been reported to participate in the process of tumorigenesis [5-8]. A previous study indicated that expression of miR-433 was downregulated in gastric cancer, according to a microRNA microarray. At the same time, low expression of miR-433 was shown to be relevant to adverse outcomes of gastric cancer [9]. Another study confirmed that miR-433 expression was decreased in advanced gastric carcinoma, suggesting that miR-433 could be an important diagnostic biomarker of gastric cancer [10]. However, the underlying mechanisms in which miR-433 participates in progression and development of gastric cancer remain largely unknown. A member of the voltage-dependent chlorine channel family, chloride channel 4

(CLCN4) had been confirmed as a novel driver of colon cancer migration, invasion, and metastases [11]. However, the roles in gastric cancer have not been fully presented.

The current study found that there was a binding site between miR-433-5p and CLCN4. Given the above evidence, this study aimed to evaluate the mechanisms of miR-433-5p in targeting CLCN4 in gastric cancer.

## Materials and methods

### *Ethical statement*

All experiments were performed in accordance with the Declaration of Helsinki. The study was approved by the Ethics Committee of the Second Hospital University of South China (HengYang, Hunan, China). Informed consent was obtained from all patients and families.

### *Bioinformatics prediction*

TargetScan7.2 ([http://www.targetscan.org/vert\\_72/](http://www.targetscan.org/vert_72/)), miRWalk (<http://mirwalk.umm.uni-heidelberg.de/>), RNA22 (<https://cm.jefferson.edu/rna22/>), and miRDB (<http://www.mirdb.org/>) were used to predict downstream genes that might have binding sites with miR-433-5p. Subsequently the intersection was chosen using Venny2.1.0 (<http://bioinfo.gp.cnb.csic.es/tools/venny/index.html>).

### *Luciferase reporter gene assay*

The 3'UTR wild type (WT) and 3'UTR-mutant (MUT) fragments of the target genes were designed and synthesized by Beijing Genomics Institute (Beijing, China). The fragments were cloned into an upstream of pmirGLO (3577193, Promega, USA). The plasmid was extracted after sequencing. HEK-293T cells (CBP60441, Cobioer, China) were cultured into 24 well plates, then co-transfected with WT or MUT CLCN4 3'UTR fragments and combined with miR-433-5p mimics and negative controls (NC), according to the instructions of Lipofectamine 3000 (L30000001, Thermo Fisher, USA). Relative luciferase activity was detected using the Dual-Luciferase Reporter assay (E2920, Promega, USA) and chemiluminescence apparatus (DX1800, Beckman Coulter, USA), after culturing for 48 hours at 37°C. Relative luciferase activity was calculated with the following formula: Luciferase activity of firefly/luciferase activity of renilla.

### *Tissue samples and cell culturing*

Gastric cancer tissues and adjacent tissues (above 4 cm from cancer focuses) of 27 patients, diagnosed at the Second Hospital University of South China, between September 2016 and October 2017, were enrolled in this study. The study consisted of 14 males and 13 females. The median age of patients was 48 years (25-76 years old). In terms of the gastric carcinoma classification, 9 cases were signet ring cell cancer, 7 cases were adeno-squamous carcinoma, 7 cases were squamous cell carcinoma, and 4 cases were undifferentiated carcinoma. A total of 24 cases were at stage I-II, while 3 cases were at III-IV, in accordance with tumor node metastasis (TNM) standards [12]. All collected tissues were cut into two pieces, with one piece fixed in 10% formaldehyde solution for pathological observation. Another piece was preserved in liquid nitrogen. MGC-803 gastric cancer cell lines were purchased from American Type Culture Collection (CC-Y1353, ATCC, USA). SGC-7901 gastric cancer cell lines were obtained from Procell (CP-H048, Procell, China). MKN-45 gastric cancer cell lines and GES-1 gastric epithelium cells were received from the Third Xiangya Hospital of Central South University (Hunan, China). Gastric cancer cell lines were cultured in RPMI 1640 medium (61870-036, ThermoFisher, USA) containing 10% fetal bovine serum. GES-1 cells were cultured with gastric mucosal epithelial cells specific culture medium (CM-H048, Procell, China).

### *Construction of gene silencing vector*

CLCN4 gene sequencing was obtained from NCBI (Accession: NM\_008561.3). CLCN4 shRNA sequences (5'-CACCGCAAGAGCAAGGAGTCCATATCGAAATATGGACTCCTTGCTCTTG-C-3') and negative control sequences (5'-CCGGCCTAAGGTTAAGTCGCTCCTCGAGGAGCG-ACTTAACCTTAGGTG-3') were designed using BLOCK-iT™ RNAi Designer. Subsequently, the two sequences were synthesized by Shenzhen BGI Health Technology Co., Ltd. (Shenzhen, China). Empty pcDNA3.1 (+) plasmid (#70219, Addgene, USA) was digested with EcoR I and BamH I restriction endonuclease. Next, the linear plasmid was extracted and constructed by ligation of CLCN4 fragments with pcDNA3.1. Subsequently, the pcDNA3.1-CLCN4 plasmid was further transfected and amplified in DH5α. The Rapid Bacterial Genomic DNA Isolation Kit

**Table 1.** Primer sequences

Gene	Forward primer(5'-3')	Reverse primer(5'-3')
CLCN4	TCTGCCTTCTGGTATAGCCAT	CAGCAGCTCCGACCATTCT
Vimentin	CTCTCAAAGATGCCCAGGAG	GCACGATCCAACCTCTTCCTC
MMP-2	TTTTCTCGAATCCATGATGG	CTGGTGCAGCTCTCATATTT
GAPDH	TGCACCACCAACTGCTTAGC	TCTTCTGGGTGGCAGTGATG

(B518225-0050, Sangon Biotech, China) was used to extract the recombinant vector after identification by agarose gel electrophoresis. The purified recombinant plasmid was preserved at -80°C.

#### Cell grouping and transfection

Gastric cancer cells were assigned into the following groups: 1) NC group (transfected with negative control sequence); 2) miR-433-5p mimic group (transfected with miR-433-5p mimic); 3) miR-433-5p inhibitor group (transfected with miR-433-5p inhibitor); 4) CLCN4 shRNA group (transfected with CLCN4 shRNA); and 5) miR-433-5p inhibitor + CLCN4 shRNA group.

**Transfection methods:** Gastric carcinoma cells at the logarithmic phase were seeded into 24-well plates. Lipofectamine 3000 (L300-0001, Thermo Fisher, USA) was used to transfect the cells until cell confluence reached 80%, in accord with manufacturer instructions. Briefly, 100 pmoL of miR-433-5p mimic was dissolved with 250 µL serum-free medium Opti-MEM, with a final concentration of 50 nM (solution A). The samples were then incubated at room temperature for 5 minutes. Next, 5 µL of Lipofectamine 3000 was dissolved with 250 µL serum-free medium Opti-MEM (solution B) and incubated at room temperature for 5 minutes. The above two solutions were mixed together and incubated at room temperature for 20 minutes. The cells were then incubated at 37°C containing 5% CO<sub>2</sub>. The RPMI1640 culture medium was changed after 6-8 hours. The cells continued to be cultured for 24-48 hours. Similar experimental steps were applied to NC sequences, miR-433-5p inhibitors, and CLCN4 shRNA.

#### H&E staining

Paraffin sections of gastric cancer and adjacent tissue samples were produced and dried

in an oven at 60°C for 1 hour. They were dewaxed using xylene I and xylene II for 5-10 minutes. The slices were hydrated using gradient ethanol (100%, 90%, 80%, 70%) for 2 minutes. The slices were washed with distilled water for 2 minutes and stained by hematoxylin for 8-10 minutes.

Subsequently, the slices were differentiated with 1% hydrochloric alcohol for 30 seconds and rinsed with running water. The slices were then immersed in eosin staining solution for 2-3 minutes, then rinsed with running water. This was followed by dehydration using gradient ethanol (90%, 80%, 70%) for 4-6 minutes. Finally, the slices were treated with xylene I and xylene II for 3-5 minutes and 5-10 minutes, respectively, and sealed with neutral gum.

#### Immunohistochemistry

Paraffin section of gastric cancer and adjacent tissue samples were obtained and dried in an oven at 60°C for 1 hour. They were dewaxed using xylene I and xylene II for 5-10 minutes. The slices were hydrated using gradient ethanol (100%, 90%, 80%, 70%, 60%, 50%, 30%) for 5 minutes. Subsequently, the slices were washed with H<sub>2</sub>O<sub>2</sub> and distilled water for 1 minute. This was followed by immersion in 95°C 0.01 M citrate solution (pH 6.0). Afterward, the slices were washed with PBS and blocked with 5% bull serum albumin (BSA) for 20 minutes. The rabbit anti-polyclonal antibody CLCN4 (1:1000, ab75008, ABCAM, UK) was added into the slices. The slices were then washed with PBS after incubating at 37°C for 20 minutes. Next, horseradish peroxidase (HRP) labeled goat anti-rabbit antibody IgG (1 µg/mL, ab-99697, ABCAM, UK) was added into the slices and incubated at 37°C for 20 minutes. The sections were washed with PBS for 3 minutes, then incubated with SABC at 37°C for 30 minutes. The slices were washed with PBS again 3 times for 5 minutes each time. Subsequently, the slices were developed with DAB, counterstained with hematoxylin, washed with running water, dehydrated with gradient ethanol, and sealed with neutral gum.

Staining intensities (SI) and positive percentages (PP) of the tissues were evaluated. SI was divided into 4 grades: Colorless, light yellow, pale brown, and tan, marked as 0, 1, 2, and 3,

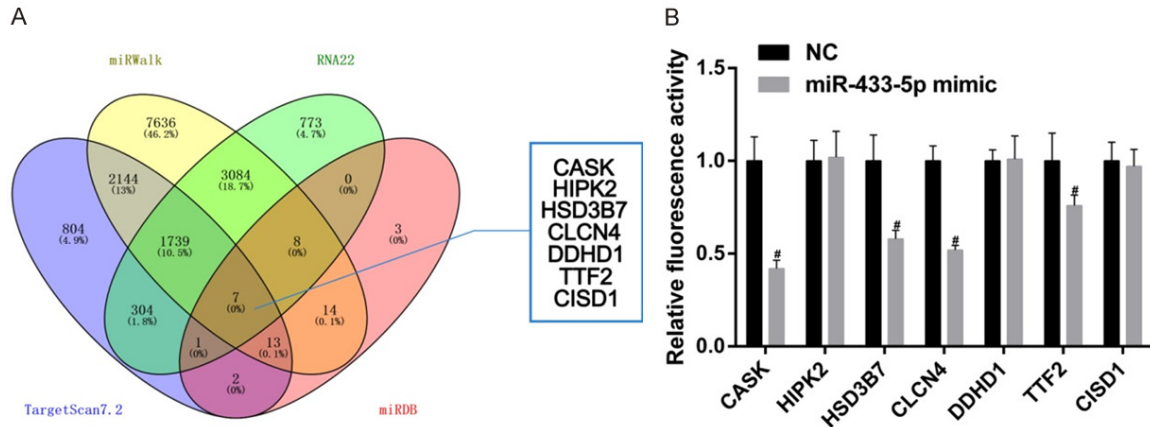


**Figure 1.** Bioinformatics tools combined with dual luciferase reporter system to predict the target gene of miR-433-5p. Note: (A) Four online prediction tools indicated that CASK, HIPK2, HSD3B7, CLCN4, DDHD1, TTF2, and CISD1 were the target genes of miR-433-5p; (B) Results obtained from dual-luciferase reporter assay system confirmed that miR-433-5p could downregulate the wild type fluorescence activity of CASK, HSD3B7, CLCN4, and TTF2. #compared with the NC group,  $P < 0.05$ .

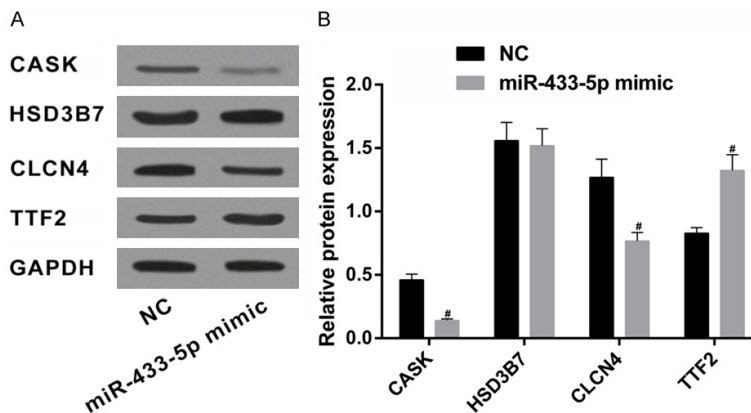


**Figure 2.** Western blotting was utilized to detect protein expression levels of target genes in SGC-7901. Note: (A) Protein bands of CASK, HSD3B7, CLCN4, and TTF2; (B) Quantification of protein expression of CASK, HSD3B7, CLCN4, and TTF2. #compared with the NC group,  $P < 0.05$ .

respectively. PP was divided into 5 grades: When positive cells were less than 5%, the slices were marked as 0. Slices were regarded as 1 when positive cells were 5%-25%. When positive cells were 25%-50%, the slices were marked as 2. Slices were regarded as 3 when positive cells were 51%-75%. When positive cells were above 75%, the slices were marked as 4. The comprehensive score was the product of SI and PP: 0 was regarded as negative; 1 was marked as weakly positive (+); 2 was marked as moderately positive (++); Slices were marked as strongly positive when the comprehensive score was more than or equal to 3 [13].

#### Reverse transcription quantitative polymerase chain reaction (RT-qPCR)

TRIzol Reagent (15596026, Invitrogen, USA) was used to extract total RNA in gastric cancer cells, in accordance with manufacturer instructions. RNA was diluted with ultra-pure water treated by diethyl phosphorocyanide (DEPC). Quality and concentrations of RNA were tested by comparing A260/280 ratios. RT-PCR and Q-PCR were conducted using the TransScript II Green One-Step qRT-PCR SuperMix kit (AQ311-01, TransGen Biotech, China).

The reaction system was as follows: 10  $\mu$ L 2  $\times$  TransStart Tip Green qPCR SuperMix, 1  $\mu$ g RNA template, 0.4  $\mu$ L of forward and reverse primer, 0.4  $\mu$ L Transcript II One-Step RT/RI Enzyme Mix, 0.4  $\mu$ L Passive Reference Dye (50  $\times$ ). Reaction conditions were: Pre-denaturation at 50°C for 5 minutes, 40-45 cycles of denaturation at 94°C for 30 seconds, 94°C for 5 seconds, annealing at 50-60°C for 5 seconds, and extension at 72°C for 10 seconds. Primers were designed and synthesized by Shenzhen BGI Health Technology Co., Ltd. (Shenzhen, China). GAPDH was used as internal reference (Table 1). Specificity and reliability of PCR results were verified by disso-



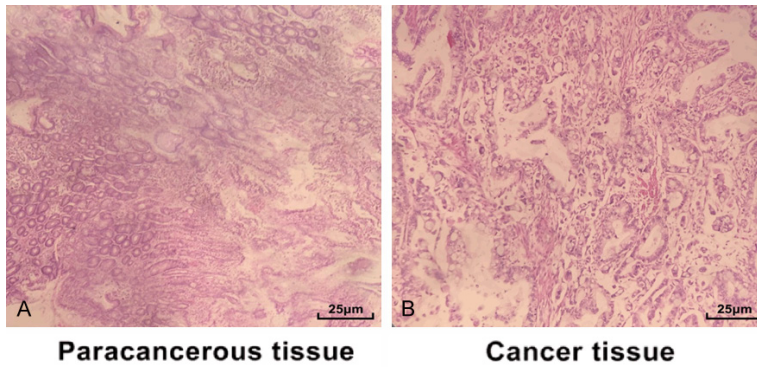


**Figure 3.** H&E staining results of gastric cancer and adjacent tissues (400 ×).

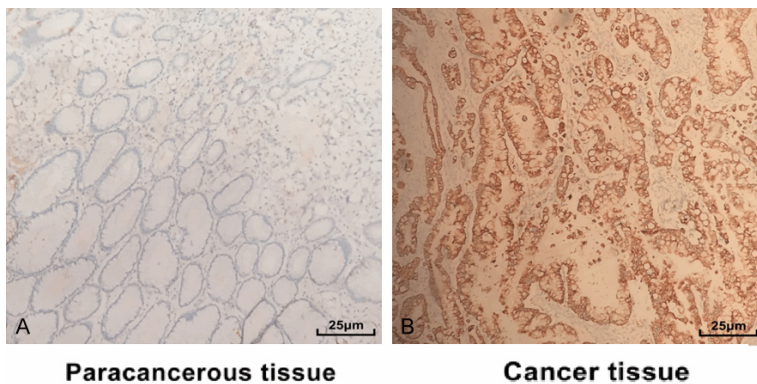


**Figure 4.** Immunohistochemistry was used to detect CLCN4 protein expression in cancer tissues and adjacent tissues (400 ×).

lution curve:  $\Delta Ct = Ct(\text{target gene}) - Ct(\text{GAPDH})$ ,  $\Delta\Delta Ct = \Delta Ct(\text{experimental group}) - \Delta Ct(\text{control group})$ . Expression of mRNA of related genes was calculated by  $2^{-\Delta\Delta Ct}$ . The experiment was repeated 3 times.

#### Western blotting

RIPA lysate (R0010, Beijing Solarbio Science & Technology Co., Ltd., China) was added to the PMSF before the experiment. The final concentration of PMSF was 1 mM. Gastric cancer cells were washed with PBS 2 times, then added with RIPA lysate ( $2.5 \times 10^7$  cells were added with 1 mL RIPA lysate). Gastric cancer cells were then incubated on ice and the lysates were centrifuged at  $12,000 \times g$  for 30 minutes. Next, protein concentrations were determined via the BCA kit (P0006, Beyotime Institute of Biotechnology, China). The proteins were transferred to PVDF membranes after separating by sodium dodecyl sulfate polyacrylamide gel electrophoresis (SDS-PAGE). The membranes were then blocked with tris buffered saline with

Tween 20 (TBST) containing 5% bovine serum albumin for 1 hour. After abandoning the blocking liquid, the membranes were incubated with primary antibody CLCN4 (1:500, ab75008, ABCAM, UK), vimentin (1:1000, ab52947, ABCAM, UK), MMP-2 (1 µg/mL, ab837150, ABCAM, UK), and GAPDH (1:1000, ab8245, ABCAM, UK). It was placed at 4°C overnight. The membranes were washed with TBST for  $3 \times 10$  minutes and incubated with goat anti-mouse IgG (1:5000, ab97040, ABCAM, UK) for 4-6 hours. Next, the membranes were washed with TBST for  $3 \times 5$  minutes. ECL (PE0010, Beijing Solarbio Science & Technology Co., Ltd., China) was used to detect the chemiluminescence signal. Target protein expression levels were quantified by determining the ratio of gray values of target protein bend to the internal reference. The experiment was repeated 3 times.

#### Cell counting kit 8 (CCK8) assay

Cells were made into the cell suspension when the cell density reached 80%. It was then added into 96-well plates with each well  $4 \times 10^3$  cells (200 µl per well). Six duplicated wells were set and cultured in an incubator. Subsequently, each well was added with 5 g/L CCK-8 solution at 24, 48, and 72 hours post-incubation. It was then incubated for another 4 hours. Each well was added with 100 µL Dimethyl sulfoxide (DMSO). A microplate reader (SpectraMax iD5, Molecular Devices, USA) was used to detect optical density (OD) values at 490 nm. Cell growth curves were made in accordance with OD values. The experiment was repeated 3 times.

#### Transwell assay

Matrigel (354230, Becton, Dickinson, and Company, USA) was diluted with serum-free MEM medium at a ratio of 1:10. The Transwell upper chamber was added with 100 µL diluted

**Table 2.** CLCN4 expression in gastric cancer tissues and adjacent tissues

	CLCN4 expression				P
	Negative (-)	Weakly positive (+)	Medium positive (++)	Strong positive (+++)	
Adjacent tissue	15	8	3	1	0.001
Gastric tissue	5	6	13	3	

Wilcoxon rank-sum tests.  $P < 0.05$  indicates statistical significance.

#### Results

*Bioinformatics prediction indicated that miR-433-5p may regulate the development of gastric cancer through targeting CLCN4*

Matrigel and placed at room temperature for 2 hours. It was rinsed with 200  $\mu$ L serum-free 1640 culture medium and resuspended using a serum-free DMEM medium. After the cells were calculated and diluted to  $3 \times 10^5$  cells/mL, 100  $\mu$ L diluted cells were added to the upper Transwell chamber. The lower chamber was added with 600  $\mu$ L DMEM containing 10% serum. After incubating for 24 hours, crystal violet staining was performed. The Transwell chambers were collected and an optical microscope (CX21, Olympus, Japan) was utilized to detect results. Invasion rate = cells passing through the Matrigel/total number of cells  $\times$  100%.

#### Annexin V-FITC/PI staining

Gastric cancer cells were washed with PBS after culturing for 48 hours. They were then centrifuged at  $2,000 \times g$  for 5 minutes. Cell density was adjusted to  $4 \times 10^5$  cells/mL after removing the supernatant. The cells were resuspended by adding with 500  $\mu$ L binding buffer. This was followed by adding 5  $\mu$ L Annexin-V-FITC and 5  $\mu$ L PI dye liquid before flow cytometry analysis. It was mixed gently and incubated in an ice bath in the dark for 10-12 minutes. Flow cytometry (CoulterCytoFLEX, Beckman Coulter, USA) was used to determine FITC and PI levels.

#### Statistical analysis

SPSS 21.0 software (IBM. Corp., Armonk, USA) was used for statistical data analysis. Quantitative data are presented as mean  $\pm$  standard deviation (SD). Each experiment was conducted in triplicate. The Kolmogorov-Smirnov method was utilized to determine the normality of data distribution in each group. Student's t-tests were used to compare group variables. One-way analysis of variance (ANOVA) was used for multiple groups analysis. LSD tests were used to compare inter-group variables. Grade data were compared using

Targetscan7.2, miRWalk, RNA22, and miRDB were used to explore potential target genes that might have binding sites with miR-433-5p. Moreover, 1,047, 14,645, 5,916, and 48 genes were identified, respectively. Venn images (**Figure 1A**) indicated that CASK, HIPK2, HSD3B7, CLCN4, DDHD1, TTF2, and CISD1 were the intersection. Subsequently, dual-luciferase reporter assays were used to confirm targeting regulatory relationships between miR-433-5p and the above genes. Results indicated that miR-433-5p have binding sites with CASK, HSD3B7, CLCN4, and TTF2 (**Figure 1B**). Next, SGC-7901 was transfected with miR-433-5p mimics. Negative controls were also set up. Western blotting was adopted to determine protein expression levels of CASK, HSD3B7, CLCN4, and TTF2. Results indicated that (**Figure 2A, 2B**), compared with the NC group, protein expression of CASK and CLCN4 was significantly downregulated. TTF2 protein expression was upregulated in the miR-433-5p mimic group (all  $P < 0.05$ ). There were no significant differences in HSD3B7 protein expression levels between NC and miR-433-5p mimic groups ( $P > 0.05$ ).

MicroRNAs always function as negative regulators in post transcriptional gene silencing (PTGS) through base pairing with target mRNAs. This results in mRNA cleavage and translational inhibition. Thus, it can be speculated that other ways may participate in the regulating effects of miR-433-5p on HSD3B7 and TTF2. Therefore, CASK and CLCN4 were selected as candidate genes in this study. The protein encoded by CASK was calcium/calmodulin dependent serine protein kinase, a member of the membrane associated guanylate kinase family. A previous study proved that CASK was highly expressed in esophageal cancer and related to progression and worse prognosis in colorectal cancer [14, 15]. In addition, CASK

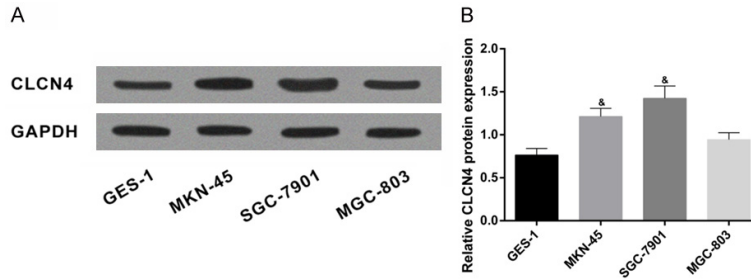


**Figure 5.** CLCN4 protein expression in different gastric cancer cells, Note: (A) The protein bands of CLCN4 in different gastric cancer cell lines; (B) Quantification of CLCN4 protein in different gastric cancer cell lines. \* $P < 0.05$ .

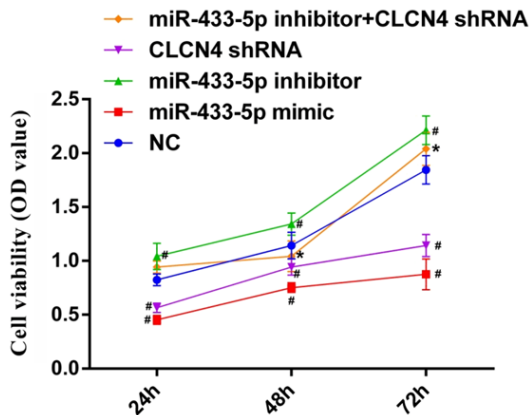


**Figure 6.** Cell viability of SGC-7901 in each group. Note: compared with NC group, \* $P < 0.05$ ; compared with miR-433-5p inhibitor group, \* $P < 0.05$ .

had been reported to participate in the growth and metastasis of gastric cancer via regulation by miR-203 [16]. Thus, the regulatory mechanisms of CASK in gastric cancer are relatively clear. CIC-4 chloride channel (CLCN4) gene is a member of voltage gated chloride channels (CICs) family. Previous studies have confirmed that CLCN4 could induce the invasion and metastasis of colon cancer using gene trapping technology. There existed gender differences in copy number variations of CLCN4 in colon cancer [11]. However, the specific molecular mechanisms of CLCN4 in gastric cancer remain largely unknown. The present study focused on the function and regulation of miR-433-5p in gastric cancer through targeting CLCN4.

#### H&E staining results

According to results obtained from H&E staining (Figure 3), gastric cancer tissues showed

histopathological changes, including a disordered and cribriform pattern of glands, absence of interstitial tissue, and glandular secretions siltation. At the same time, the glandular cavity was integrated into expansion and size of cysts. Regarding the para-cancerous tissues, the nucleus was occasionally found and appeared as signet ring form. The nuclear membrane was thickened. The cancer tissue invaded the gastric fundus glandular mucosa.

#### CLCN4 expression was upregulated in gastric cancer

Immunohistochemical staining was performed to examine expression of CLCN4 in tumor tissues and para-cancerous tissues. Results showed that (Figure 4, Table 2) CLCN4 was mainly expressed in signet cells, as well as the cytoplasm and nucleolus. Compared to adjacent normal tissues, elevated CLCN4 expression was found in cancer tissues.

#### Highest levels of CLCN4 found in SGC-7901 cells

Western blotting was utilized to detect CLCN4 expression. Results indicated that (Figure 5), compared with GES-1, levels of CLCN4 in other cell lines were significantly upregulated. The highest level of CLCN4 expression was found in SGC-7901 cell lines. Thus, SGC-7901 was selected for the experiments.

#### miR-433-5p inhibited cell viability of SGC-7901 through targeting CLCN4

To evaluate the impact of miR-433-5p in SGC-7901 cell line, cells were transfected with miR-433-5p inhibitors, miR-433-5p mimics, or CLCN4 shRNA. CCK-8 assays were performed to determine the cell viability in each group. Results indicated that (Figure 6), compared with the NC group, cell viability was significantly decreased after the cells were transfected with miR-433-5p mimics or CLCN4 shRNA, at each time point (all  $P < 0.05$ ). However, cell viability in the miR-433-5p inhibitor group was obviously increased, compared with the NC group.



## Effects of miR-433-5p and CLCN4 in gastric cancer

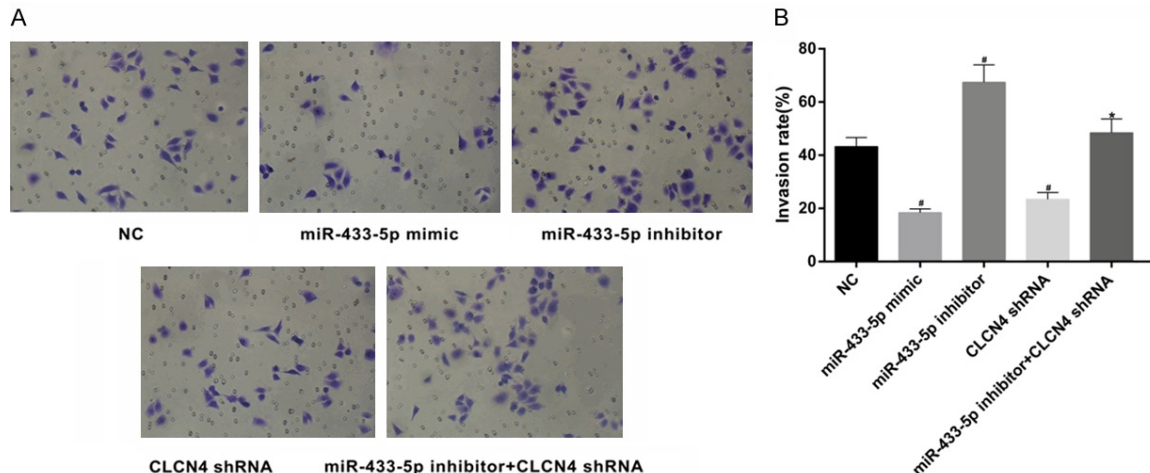


**Figure 7.** Invasion ability of SGC-7901 in each group. Note: (A) Transmembrane cells stained by crystal violet in each group; (B) Quantification of invasive rate in each group. Compared with NC group,  $^{\#}P < 0.05$ ; compared with miR-433-5p inhibitor group,  $^{*}P < 0.05$ .

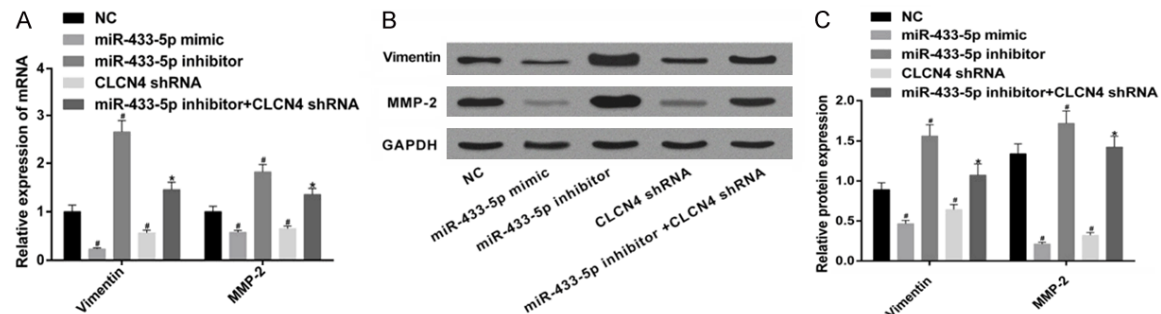


**Figure 8.** mRNA and protein expression of vimentin and MMP-2 in each group of SGC-7901 cell. Note: (A) mRNA expression of vimentin and MMP-2 in each group; (B) Protein bands of vimentin and MMP-2 in each group; (C) Quantification of vimentin and MMP-2 protein expression in each group. Compared with NC group,  $^{\#}P < 0.05$ ; compared with miR-433-5p inhibitor group,  $^{*}P < 0.05$ .

Effects of miR-433-5p inhibitors on SGC-7901 cells can be reversed by silencing of CLCN4.

### *miR-433-5p inhibited invasion and metastasis of SGC-7901 by targeting CLCN4*

Transwell assays were adopted to determine invasion abilities in each group. Results revealed that (Figure 7), compared with the NC group, invasion abilities of the miR-433-5p mimic group and CLCN4 shRNA group were significantly decreased (all  $P < 0.05$ ). However, invasion abilities in the miR-433-5p inhibitor group were obviously enhanced ( $P < 0.05$ ). Moreover, CLCN4 silencing could reverse tumor invasion induced by miR-433-5p inhibitors.

Western blotting and Q-PCR were performed to quantify the mRNA and protein expression lev-

els of vimentin and MMP-2. Results indicated that (Figure 8), compared with the NC group, vimentin and MMP-2 mRNA and protein expression levels were significantly downregulated in the miR-433-5p mimic group and CLCN4 shRNA group (all  $P < 0.05$ ). However, levels in the miR-433-5p inhibitor group were obviously upregulated ( $P < 0.05$ ). CLCN4 silencing could partly reverse the induction of vimentin and MMP-2 induced by miR-433-5p inhibitors.

### *miR-433-5p could promote SGC-7901 apoptosis through targeting CLCN4*

Annexin V-FITC/PI staining was utilized to detect apoptosis levels of SGC-7901 in each group. Results obtained from this experiment indicated that (Figure 9), compared with the NC group, SGC-7901 apoptosis was significantly increased



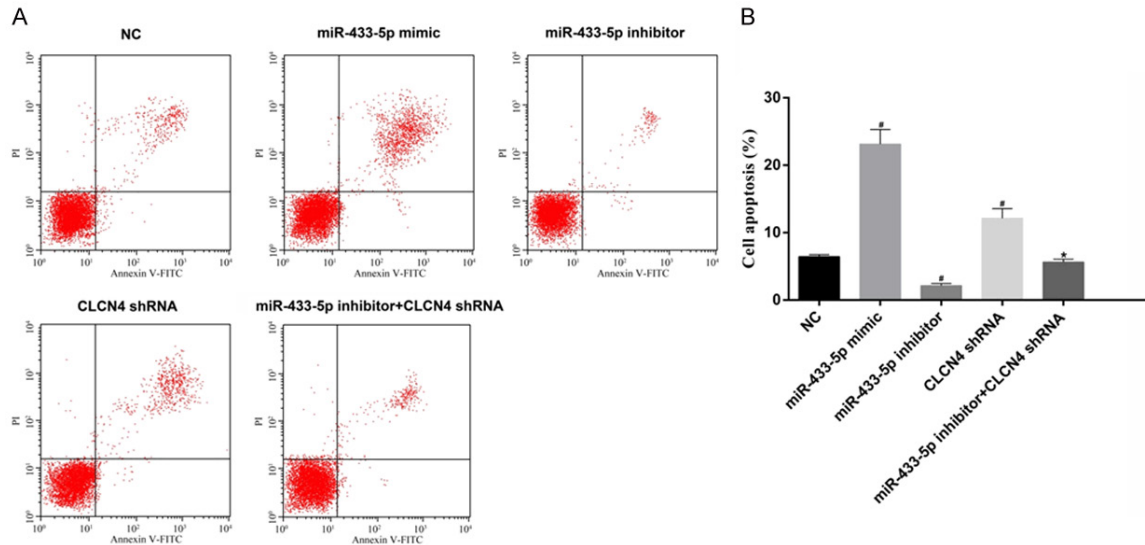


**Figure 9.** Apoptosis of SGC-7901 cells in each group. Note: (A) SGC-7901 cell apoptosis in each group was determined by Annexin V-FITC/PI staining; (B) Quantification of SGC-7901 cell apoptosis rates in each group. Compared with NC group,  $^{\#}P < 0.05$ ; compared with miR-433-5p inhibitor group,  $^{*}P < 0.05$ .

in the miR-433-5p mimic group and CLCN4 shRNA group (all  $P < 0.05$ ). However, cell apoptosis was inhibited when cells were transfected with miR-433-5p inhibitors. CLCN4 silencing could partly reverse SGC-7901 apoptosis induced by miR-433-5p inhibitors.

## Discussion

Prognosis of patients with advanced gastric cancer remains extremely low despite great advancements made in targeting preparations and cytotoxic drugs [17-19]. Thus, it is important to reveal the underlying pathological mechanisms of gastric carcinoma, providing novel diagnostic biomarkers and new strategies for gastric cancer therapy. Moreover, miR-433 has been reported to play a significant role in the progression of gastric carcinoma [10]. Guo LH et al. confirmed that miR-433 exerted a suppressor role in gastric cancer [20]. Thus, the current study focused on miR-433-5p and its potential mechanisms in gastric cancer. A series of experiments were performed. Results obtained from this study indicate that miR-433-5p could inhibit viability, as well as invasion and metastasis, of gastric cancer cells. It may also induce cell apoptosis through downregulation of CLCN4.

Initially, bioinformatics tools and dual-luciferase reporter assays were used to predict the

target genes of miR-433-5p. CLCN4 was eventually selected. A study designed by Ishiguro et al. found that CLCN4 could induce invasion and metastasis of colon cancer [11]. Thus, this study focused on roles in gastric cancer. Evidence obtained from immunohistochemical tests demonstrated that CLCN4 expression was upregulated in gastric cancer tissues, compared with para-cancerous tissues. SGC-7901 cell lines were used for subsequent experiments and transfected with miR-433-5p mimics, miR-433-5p inhibitors, or CLCN4 shRNA. CCK8 assay and Transwell assay results proved that miR-433-5p overexpression or CLCN4 silencing could inhibit the viability and invasion abilities of gastric cancer cells. Metastasis and recurrence are the most important factors that affect the prognosis of cancer patients. Degradation of the basement membrane is a key point for tumor metastasis and invasion [21-23]. Matrix metalloproteinases (MMPs), a calcium-dependent endopeptidase, has been proven to have the ability to degrade the extracellular matrix, promoting metastasis and invasion of tumors [24-27]. MMP2 is an important member of the MMPs family. In this study, it was found that mRNA and protein expression levels of MMP-2 were significantly decreased after SGC-7901 cell lines were transfected with miR-433-5p mimics or CLCN4 shRNA. CLCN4 silencing could partly reduce MMP2 expression induced by miR-433-5p inhibitors. Vimentin is

a kind of cytoskeletal protein. Accumulating evidence has demonstrated that vimentin is expressed in a variety of tumor cells [28-31]. Detection of vimentin expression has been an important measure in diagnosing or screening of cancer [32, 33]. Results also confirmed that miR-335-5p could downregulate expression of vimentin through inhibition of CLCN4. Annexin V-FITC/PI staining results showed that, compared with the NC group, cell apoptosis was increased in the miR-433-5p mimic group and CLCN4 shRNA group, while decreased in the miR-433-5p inhibitor group. Present results suggest that miR-433-5p could promote cell apoptosis by inhibiting CLCN4.

Collectively, key findings obtained in this study indicate that miR-433-5p can act as a tumor suppressor in gastric cancer. It can inhibit gastric cancer cell viability, invasion, and metastasis. At the same time, it may induce gastric cancer cell apoptosis through downregulation of CLCN4. Current findings demonstrate the vital roles of miR-433-5p and CLCN4 in gastric cancer, suggesting that miR-433-5p and CLCN4 could serve as a pivotal therapeutic targets in gastric cancer management. More *in vivo* and *in vitro* studies are necessary to further validate the clinical utility.

## Disclosure of conflict of interest

None.

**Address correspondence to:** Hai-Bing Jiang, Department of Gastroenterology, The Second Hospital University of South China, No.35 Jiefang Avenue, Huaxin Development Zone, Hengyang 421001, China. Tel: 0734-8899680; E-mail: haibingjiang680@163.com

## References

- [1] Hu B, Wang B, Zhao B, Guo Q, Li ZH, Zhang XH, Liu GY, Liu Y, Tang Y, Luo F, Du Y, Chen YX, Ma LY and Liu HM. Thiosemicarbazone-based selective proliferation inactivators inhibit gastric cancer cell growth, invasion, and migration. *Medchemcomm* 2017; 8: 2173-2180.
- [2] Coburn N, Cosby R, Klein L, Knight G, Malthaner R, Mamazza J, Mercer CD and Ringash J. Staging and surgical approaches in gastric cancer: a systematic review. *Cancer Treat Rev* 2018; 63: 104-115.
- [3] Wang W, Li Z, Wang J, Du M, Li B, Zhang L, Li Q, Xu J, Wang L, Li F, Zhang D, Xu H, Yang L, Gong W, Qiang F, Zhang Z and Xu Z. A functional polymorphism in TFF1 promoter is associated with the risk and prognosis of gastric cancer. *Int J Cancer* 2018; 142: 1805-1816.
- [4] Dugue PA, Bassett JK, Joo JE, Jung CH, Ming Wong E, Moreno-Betancur M, Schmidt D, Makalic E, Li S, Severi G, Hodge AM, Buchanan DD, English DR, Hopper JL, Southey MC, Giles GG and Milne RL. DNA methylation-based biological aging and cancer risk and survival: Pooled analysis of seven prospective studies. *Int J Cancer* 2018; 142: 1611-1619.
- [5] Zhang X, Li Z, Xuan Z, Xu P, Wang W, Chen Z, Wang S, Sun G, Xu J and Xu Z. Novel role of miR-133a-3p in repressing gastric cancer growth and metastasis via blocking autophagy-mediated glutaminolysis. *J Exp Clin Cancer Res* 2018; 37: 320.
- [6] Daneshpour M, Karimi B and Omidfar K. Simultaneous detection of gastric cancer-involved miR-106a and let-7a through a dual-signal-marked electrochemical nanobiosensor. *Biosens Bioelectron* 2018; 109: 197-205.
- [7] Zhang H, Mao F, Shen T, Luo Q, Ding Z, Qian L and Huang J. Plasma miR-145, miR-20a, miR-21 and miR-223 as novel biomarkers for screening early-stage non-small cell lung cancer. *Oncol Lett* 2017; 13: 669-676.
- [8] Chen YL, Xu QP, Guo F and Guan WH. MicroRNA-302d downregulates TGFBR2 expression and promotes hepatocellular carcinoma growth and invasion. *Exp Ther Med* 2017; 13: 681-687.
- [9] Ueda T, Volinia S, Okumura H, Shimizu M, Taccioli C, Rossi S, Alder H, Liu CG, Oue N, Yasui W, Yoshida K, Sasaki H, Nomura S, Seto Y, Kaminishi M, Calin GA and Croce CM. Relation between microRNA expression and progression and prognosis of gastric cancer: a microRNA expression analysis. *Lancet Oncol* 2010; 11: 136-146.
- [10] Luo H, Zhang H, Zhang Z, Zhang X, Ning B, Guo J, Nie N, Liu B and Wu X. Down-regulated miR-9 and miR-433 in human gastric carcinoma. *J Exp Clin Cancer Res* 2009; 28: 82.
- [11] Ishiguro T, Avila H, Lin SY, Nakamura T, Yamamoto M and Boyd DD. Gene trapping identifies chloride channel 4 as a novel inducer of colon cancer cell migration, invasion and metastases. *Br J Cancer* 2010; 102: 774-782.
- [12] Shparyk IaV. [New classification of malignant tumors TNM (5th edition)]. *Klin Khir* 1998; 36-38.
- [13] Konno R, Yamakawa H, Utsunomiya H, Ito K, Sato S and Yajima A. Expression of survivin and Bcl-2 in the normal human endometrium. *Mol Hum Reprod* 2000; 6: 529-534.
- [14] Wei JL, Fu ZX, Fang M, Zhou QY, Zhao QN, Guo JB, Lu WD and Wang H. High expression of

- CASK correlates with progression and poor prognosis of colorectal cancer. *Tumour Biol* 2014; 35: 9185-9194.
- [15] Wang Q, Lu J, Yang C, Wang X, Cheng L, Hu G, Sun Y, Zhang X, Wu M and Liu Z. CASK and its target gene Reelin were co-upregulated in human esophageal carcinoma. *Cancer Lett* 2002; 179: 71-77.
- [16] Lozovatsky L, Abayasekara N, Piawah S and Walther Z. CASK deletion in intestinal epithelia causes mislocalization of LIN7C and the DLG1/Scrib polarity complex without affecting cell polarity. *Mol Biol Cell* 2009; 20: 4489-4499.
- [17] Zhong J, Zhao W, Ren F, Qi S, Wang X, Lv T, Su Z, Yin H, Ren J and Huan Y. Lymph node metastasis in patients with gastric cancer: a multimodality, morphologic and functional imaging study. *Am J Transl Res* 2016; 8: 5601-5609.
- [18] Lee MH, Cho Y, Kim DH, Woo HJ, Yang JY, Kwon HJ, Yeon MJ, Park M, Kim SH, Moon C, Tharmalingam N, Kim TU and Kim JB. Menadione induces G2/M arrest in gastric cancer cells by down-regulation of CDC25C and proteasome mediated degradation of CDK1 and cyclin B1. *Am J Transl Res* 2016; 8: 5246-5255.
- [19] Ito H, Sato J, Tsujino Y, Yamaguchi N, Kimura S, Gohda K, Murakami K, Onimaru M, Ohmori T, Ishikawa F and Inoue H. Long-term prognostic impact of circulating tumour cells in gastric cancer patients. *World J Gastroenterol* 2016; 22: 10232-10241.
- [20] Guo LH, Li H, Wang F, Yu J and He JS. The tumor suppressor roles of miR-433 and miR-127 in gastric cancer. *Int J Mol Sci* 2013; 14: 14171-14184.
- [21] Zhang L, Kim S, Ding W, Tong Y, Zhang X, Pan M and Chen S. Arsenic sulfide inhibits cell migration and invasion of gastric cancer in vitro and in vivo. *Drug Des Devel Ther* 2015; 9: 5579-5590.
- [22] Xu X, Chen L, Xu B, Xie Q, Sun M, Deng X, Wu C and Jiang J. Increased MT2-MMP expression in gastric cancer patients is associated with poor prognosis. *Int J Clin Exp Pathol* 2015; 8: 1985-1990.
- [23] Kosaka Y, Mimori K, Fukagawa T, Ishikawa K, Etoh T, Katai H, Sano T, Watanabe M, Sasako M and Mori M. Clinical significance of molecular detection of matrix metalloproteinase-1 in bone marrow and peripheral blood in patients with gastric cancer. *Ann Surg Oncol* 2012; 19 Suppl 3: S430-437.
- [24] Torres-Martinez AC, Gallardo-Vera JF, Lara-Holgún AN, Montano LF and Rendon-Huerta EP. Claudin-6 enhances cell invasiveness through claudin-1 in AGS human adenocarcinoma gastric cancer cells. *Exp Cell Res* 2017; 350: 226-235.
- [25] Wang Z, Li G, Wu H, Sun K, Chen J, Feng Y, Chen C, Cai S, Xu J and He Y. CXCL1 from tumor-associated lymphatic endothelial cells drives gastric cancer cell into lymphatic system via activating integrin beta1/FAK/AKT signaling. *Cancer Lett* 2017; 385: 28-38.
- [26] Wei Y, Zhao L, He W, Yang J, Geng C, Chen Y, Liu T, Chen H and Li Y. Benzo [a] pyrene promotes gastric cancer cell proliferation and metastasis likely through the Aryl hydrocarbon receptor and ERK-dependent induction of MMP9 and c-myc. *Int J Oncol* 2016; 49: 2055-2063.
- [27] Xu J, E C, Yao Y, Ren S, Wang G and Jin H. Matrix metalloproteinase expression and molecular interaction network analysis in gastric cancer. *Oncol Lett* 2016; 12: 2403-2408.
- [28] Kumar C, Rasool RU, Iqra Z, Nalli Y, Dutt P, Satti NK, Sharma N, Gandhi SG, Goswami A and Ali A. Alkyne-azide cycloaddition analogues of dehydrozingerone as potential anti-prostate cancer inhibitors via the PI3K/Akt/NF- $\kappa$ B pathway. *Medchemcomm* 2017; 8: 2115-2124.
- [29] Xu ZF, Sun XK, Chen G, Han C, Wang F and Zhang YD. Oroxyloside inhibits human glioma progression by suppressing proliferation, metastasis and inducing apoptosis related pathways. *Biomed Pharmacother* 2018; 97: 1564-1574.
- [30] Zheng P, Li H, Xu P, Wang X, Shi Z, Han Q and Li Z. High lncRNA HULC expression is associated with poor prognosis and promotes tumor progression by regulating epithelial-mesenchymal transition in prostate cancer. *Arch Med Sci* 2018; 14: 679-686.
- [31] Shi W, Wang X, Ruan L, Fu J, Liu F and Qu J. MiR-200a promotes epithelial-mesenchymal transition of endometrial cancer cells by negatively regulating FOXA2 expression. *Pharmazie* 2017; 72: 694-699.
- [32] Li MY, Liu JQ, Chen DP, Li ZY, Qi B, Yin WJ and He L. p68 prompts the epithelial-mesenchymal transition in cervical cancer cells by transcriptionally activating the TGF- $\beta$ 1 signaling pathway. *Oncol Lett* 2018; 15: 2111-2116.
- [33] Wu F, Zhu J, Mao Y, Li X, Hu B and Zhang D. Associations between the epithelial-mesenchymal transition phenotypes of circulating tumor cells and the clinicopathological features of patients with colorectal cancer. *Dis Markers* 2017; 2017: 9474532.